The Eurasia Proceedings of Science, Technology, Engineering & Mathematics (EPSTEM)
ISSN: 2602-3199

The Eurasia Proceedings of Science, Technology, Engineering and Mathematics (EPSTEM), 2025

Volume 37, Pages 614-628

ICEAT 2025: International Conference on Engineering and Advanced Technology

Effect of Blades Shape and Duct Geometrical Parameters on Aerodynamic Performance of a Small-Sized Axial Fan

Saddam Mansi
Al-Furat Al-Awsat Technical University

Balasem Abdulameer Jabbar
Al-Furat Al-Awsat Technical University

Abstract: Axial flow fans are vital in sectors such as civil, automotive, and electronic systems, where their improved performance can significantly increase fan efficiency, reduce operating costs, and minimize environmental impact. This study aims to analyze the geometric design factors affecting the performance of a small axial flow fan using experimental and numerical approaches. The study investigates the number of blades, blade shape, and shroud configuration to optimize these parameters for maximum air speed and flow rate. The experimental setup involves a customized open inlet/outlet duct design with a small axial fan mounted at its intermediate portion. Flow characteristics are measured at 17 selected points across the inlet. A three-dimensional computational fluid dynamics (CFD) model is developed using ANSYS 2020 R2 to evaluate the time-averaged performance under quasi-steady conditions by solving the RANS equations for steady, incompressible, and turbulent flow. The SST k-ω turbulence model is used to capture turbulent kinetic energy and predict flow separation under opposing pressure gradients. The model was validated against experimental data, demonstrating excellent agreement, confirming its reliability in fan design optimization. Numerical results confirmed the seven-blade fan's superior performance over the two basic six-blade designs and the proposed five-blade design. The seven-blade fan design was then further optimized by evaluating eight distinct blade design variations, achieving a 3.5% improvement in flow velocity. The optimized seven-blade fan design was then used in the shroud design optimization process, achieving an 11% improvement in flow velocity.

Keyword: Axial flow fan, Blade optimization, Shroud design

Introduction

Axial flow fans are broadly employed in civil, technical, and electronic systems, including air ventilation, vehicles, and power plants, due to their compact size, affordable cost, and high flow rate. Despite their widespread use, small-sized axial fans suffer from inefficiencies due to suboptimal blades and shroud designs, leading to energy losses. This study aims to optimize blade number, shape, and shroud geometry to improve airflow speed and efficiency. The extensive use of axial fans in suboptimal conditions highlights significant potential for performance enhancement, which could reduce global energy consumption. In this context, numerous studies have recently been conducted to enhance performance using various approaches. Flow control strategies are used to enhance the leading and trailing edges (Corsini et al., 2015), investigating the tip clearance effects, and the investigation of the blade number effect (Yadegari et al., 2024). On the other hand, optimization methods, using Computational Fluid Dynamics (CFD), are widely adopted for the fan design parameters optimization process. Optimizing blade shape

plays a vital role in improving the performance of turboprop engines. In compact axial fan systems, high pressure often leads to excessive tip leakage and increased vortex generation. To address these issues, blade designs must be tailored to the tip-to-shroud gap dimensions, highlighting the importance of optimization strategies in axial fan research. In this context, several studies have been conducted recently, including (but not limited to) (Ryu et al., 2024; Sun et al. 2024; Qiao et al., 2025).

Tutar and Cam (2025) present a conceptual design for a small axial-flow propeller, considering the individual and combined effects of the small wing and the pitch angle on performance under various operating conditions using computational fluid dynamics. The results show that combining a +10° pitch angle with a small wing with a 6.77 mm curvature and -7° roll significantly improves efficiency. In another study conducted by Moghadam et al. (2019), a large vortex simulation study was conducted on a rated axial fan. The results showed that increasing the tip gap size ($s/D_0 = 0.001–0.01$) enhanced the tip leakage vortices and reduced the efficiency. The large-eddy simulation was also implemented in a study conducted by Park, Choi et al. (2019) to examine the effect of shroud enclosure on leakage flow. The study proposed a shroud enclosure near the trailing edge, which under design conditions efficiently blocked the tail leakage and weakened the leakage vortex, improving efficiency. However, while the enclosure improved the aerodynamic performance at the design points and maximum efficiency, performance decreased under overflow conditions. Liu et al. (2023) studied the effect of fan tip clearance on performance through experiments and simulations. The results showed that large fan tip clearance significantly reduces fan efficiency. With the same objective, a study conducted by Chen et al. (2025) focused on how diverse flow rates influence tip leakage patterns. Tip leakage dominates flow near the blade tips above 1.0 Q_{BEP} (flow rate at the best efficiency point), while lower flow rates introduce leading-edge overflow. The interaction between tip leakage, leading-edge overflow, and inlet backflow arose as the key contributors to energy loss within the tip clearance region. Tip clearance was also considered by Vala et al. (2024) who provided tip clearance and volumetric flow rate optimization. Peak performance was reported at a 1 mm tip clearance and a flow rate of 10.74 m^3/s.

A numerical approach is essential for the accurate investigation of tip leakage losses, enabling accurate evaluation of flow behavior and performance that are difficult to perform experimentally. In this regard, Meyer et al. (2022) developed a numerical approach that combines design of experiments, Kriging-based surrogate modeling, and efficient global optimization (EGO) to optimize parameters. The results showed that the optimized design increased the total-to-static pressure rise by 32.90% and improved the total-to-static efficiency by 7.66%. Kong, Wang et al. (2023) used a surrogate-assisted computational fluid dynamics (CFD) approach combined with kriging models and a genetic algorithm to guide the optimization. The results showed an efficiency improvement of up to 5.47%, with reduced tip leakage severity and improved pressure distribution. More recently, Amin, Salunkhe et al. (2024) combined Taguchi method for optimization and unsteady simulations with the SST turbulence model to investigate trapezoidal slotted casing to improve the stall margin. Results reported a 23.4% stall margin increase and a 0.54% pressure rise. Neshat (2024) proposed a numerical approach, consisting of CFD, fluid-structure interaction (FSI), and rigid body motion techniques, where CFD aims to evaluate leakage flow characteristics, while FSI aims to model rotor deformation. The literature review reveals a clear gap in understanding how blade number, shape, and shroud angle collectively affect axial fan performance. Unlike prior studies focusing on isolated parameters, this work investigates the combined effects of blade and shroud design which intends to improve the overall aerodynamic performance of small-scale axial fans.

Methodology

Experimental Setup

This section details the fan test facility employed to conduct the experiments, which also functions as the basis for the simulation study. The tests were conducted at the Engineering Laboratories of Al-Najaf Technical College, Al-Furat Al-Awsat Technical University. A glass duct was utilized in experiments specifically designed with open inlet and outlet sections with dimensions of 90 cm in length 30×30 cm for cross section as illustrated in Figure 1. A six-blade Toshiba compact axial flow fan (model VRH20J10) is employed in the experiment due to its widespread use in variety of applications. It is used as a reference case study which is considered as a Baseline Model (BM) for all subsequent modifications and development throughout the study. As the Fan is used for exhaust purposes, it was installed at 40 cm from the duct inlet with 17 designated measurement points at inlet to evaluate the performance by measuring the air velocity at these points. The air velocity data were captured using a UNI-T

micro-anemometer (model UT363BT). The average inlet velocity was measured at 2.2 m/s, resulting in a mass flow rate of 0.223 m³/s. The test was conducted at an ambient temperature of 22°C, with the effects of temperature changes neglected.

Figure 1. Experimental setup device. (1-outlet 2- plastic glass 3- shroud 4- axial fan 5- inlet 6- Iron scale)

Simulation Work

Numerical simulation has become an essential and effective tool in engineering analysis. In studies of axial flow fans, simulation approaches have been widely used to improve performance and optimize engineering. Through accurate simulation, modeling enables estimation of performance under a variety of conditions, significantly reducing the need for expensive physical prototypes. Furthermore, simulation enables engineers to perform optimizations that help optimize fan blade configurations, shroud designs, and other geometric parameters to achieve higher efficiency.

The Baseline Geometry Model of Fan and Shroud

Using invers design technique, the geometrical configuration of the BM (fan and shroud) were modeled using SolidWorks in order to develop it. As BM model included the base fan (A) and base shroud (S1) so, these geometrical parameters presented in Figure 2 and Shroud)

.

Table 1. Axial fan and shroud characteristics

Characteristic	Value
Number of fan blades	6
Diameter of fan hub (D_h) (cm)	9.5
Diameter of fan Tip (D t) (cm)	21
Speed (r p m)	1042
Average velocity inlet (m /s)	2.2
flow rate (m^3 /s)	0.223
Air inlet diameter of shroud (Ri) (cm)	25.9
Air outlet diameter of shroud (Ro) (cm)	22.4
length shroud (DL) (cm)	7

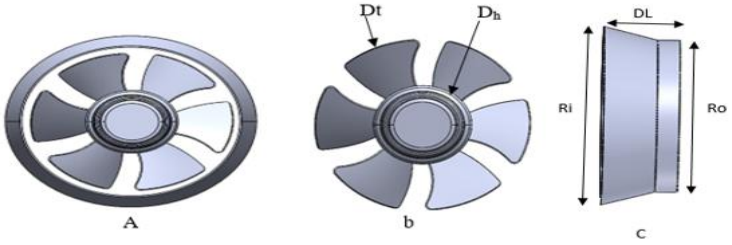

Figure 2. Fan and shroud model design (a - Fan and shroud, b- Fan, c- Shroud)

Governing Flow Equations

ANSYS CFX software was used to solve these equations, and a high-resolution second-order numerical model was presented using the finite volume method on a small-scale axial fan. The shear stress transport (SST) model was chosen as the turbulence model because it has good properties. This two-equation eddy viscosity model builds on the respective capabilities of the k-ε model for free-stream flow and the k-ω model, based on the turbulent kinetic energy transfer equation in the rotor boundary layer. This model integrates the k-ω mode used near the walls with the k-ε model away from the near-wall region (Dragomirescu, 2011; Roy & Saha, 2013). Among these conservation equations, the mass balance equation is used. Based on previous studies (Akwa et al. 2012) and (Sharma and Sharma 2016), equation (1) in the notation represents the mass balance, where $\bar{u}_i$ is the average airflow velocity, $\acute{u}_i$ is the velocity fluctuation due to turbulence effects, and x represents the flow direction.

$$\frac{\partial}{\partial x_i}(\bar{u}_i + \grave{u}_i) = 0 \tag{1}$$

where $\bar{u}_i$= average velocity of air flow; $\grave{u}_i$=velocity fluctuation due to turbulence effects; x=direction of flow. The momentum equation must be solved in conjunction with the mass balance equation. Equation (2) represents the momentum equation:

$$\frac{\partial \overline{u_i}}{\partial t} + \overline{u_j}\frac{\partial \overline{u_i}}{\partial x_j} = -\frac{1}{\rho}\frac{\partial \bar{p}}{\partial x_i} + \frac{\mu}{\rho}\frac{\partial^2 \overline{u_i}}{\partial x_i \partial x_j} - \frac{\partial y}{\partial x_j}\overline{\acute{u}_i \acute{u}_j} \tag{2}$$

where t is time, $\bar{p}$ is the average pressure, ρ is the density, and μ is the dynamic viscosity of atmospheric air.

Simulation Domain and Boundary Conditions

A similar three -dimensional fan model is created with an experimental setting. With the creation of a field to repeat the experimental composition that includes a rectangular channel. The field of flow is two areas: the fixed area and the rotating area, as shown in the Figure 3, the fixed area is a flow field consisting of three sections: the entrance and exit sections, whose walls are fixed, each of which is 41.5 cm, a width of 30 cm, and a height of 30 cm. The third section, located in the middle of the road between the entrance and exit sections, contains dimensions that meet the dimensions of the fan cover: 25.8 cm on the side of the entrance, and its diameter is 22.4 cm on the side of the exit, and its height is 7 cm. Its walls are fixed. The rotating area is placed inside the fixed area with rotational engineering at the origin of the coordinate system, with a diameter of 21.5 cm and a height of 1 cm. Its walls are fixed and unchangeable. The dimensions of the field of arithmetic flow and comparison with those in the experimental study have been identified. The boundaries of the fixed area were defined as the air inlet and outlet, while the remaining walls were treated as stationary. The rotating area walls were set as moving boundaries.

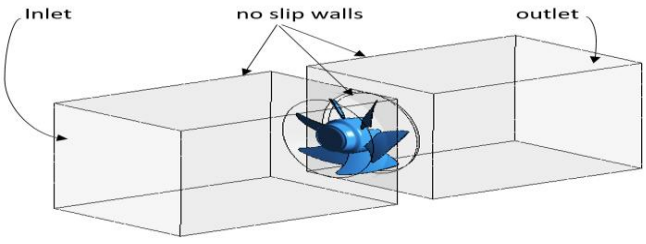

Figure 3. Simulation domain of the axial-flow fan.

Mesh and Grid Independence

The computational mesh was generated in ANSYS CFX using unstructured 3D tetrahedral meshing due to its flexibility in handling complex geometries. The tetrahedral elements were employed for both the rotating and stationary domains, as illustrated in Figure . A fine mesh with a growth rate of 1.2 was applied, and five blowing

layers were created on the rotor surface, based on the thickness of the first layer selected. Based on previous studies (Sharma & Sharma 2016; Ostos et al., 2019), the distance of the first node from the wall, y+, was calculated, using Equation.3, as the ratio of turbulent and laminar effects in the cell.

$$y^+ = \frac{\rho U_t y}{\mu} \quad (3)$$

where + (1) y is a no dimensional parameter, U t is the friction velocity, ρ is f fluid density, μ is the fluid viscosity; and y is the distance from the wall to the first node.

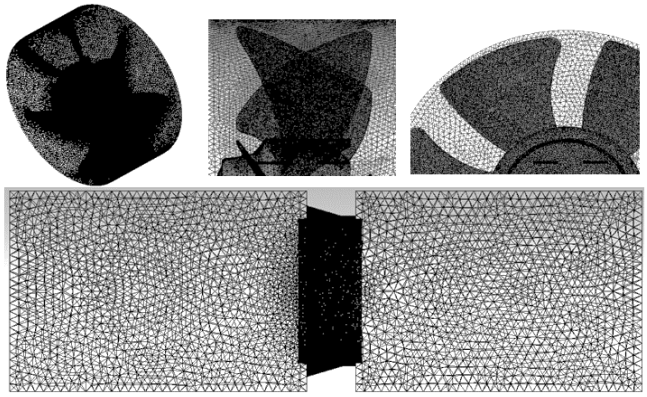

Figure 4. Simulation mesh details

Table 3 also shows the percentage error between the measured and calculated air velocity values. To assess the numerical accuracy of the model, retinal sizes have been investigated. Figure 5 shows the choice of the Mesh3, the fact that the flow speed in the points designated for the entrance is close to experimentally measured data with an increase in the intensity of the network.

Table 2, present the mesh quality evaluation in terms of skewness for the domain at a flange. This mesh was selected not only for yielding accurate results with the fewest elements but also for its lower computational cost. Table 3 also shows the percentage error between the measured and calculated air velocity values. To assess the numerical accuracy of the model, retinal sizes have been investigated. Figure 5 shows the choice of the Mesh3, the fact that the flow speed in the points designated for the entrance is close to experimentally measured data with an increase in the intensity of the network.

Table 2. The statistics of grid independence

Trial	Elements. No. (Rotary) And (Stationary)	Node No. (Rotary) And (Stationary)	Skewness (Rotary)	Skewness (Stationary)	Orthogonal Quality (Rotary)	Orthogonal Quality (Stationary)
1	1276713	241105	0.7651	0.75112	0.99063	0.99478
2	2570813	478816	0.75784	0.76484	0.99392	0.99427
3	5143094	943694	0.70771	0.7087	0.99655	0.99393
4	7201170	1335749	0.7951	0.75112	0.99588	0.99478

Table 3. The error rate between the measured air velocity value and the calculated values.

Trial	Measured value of air velocity	Calculated values	Error%
1	2.2	2.040	7.1%
2	2.2	2.073	5.64%
3	2.2	2.076	5.54%
4	2.2	2.054	6.49%

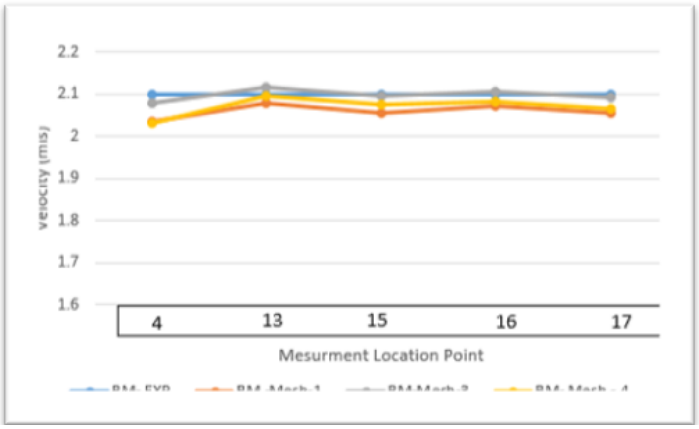

Figure 4. The mesh refinement effect on the determined velocity compared to experimentally measured values

Development of BM Mode

Blade Number Assessment

The analysis in this section evaluates how the number of blades affect flow velocity by comparing three fan models with different blade numbers. The basic six-blade fan was used as a reference, while alternative five- and seven-blade models, with the same blade design, were analyzed to evaluate performance differences. For clarity, the fan models are plotted as follows: A for the basic six-blade model, B for the five-blade model, and F for the seven-blade model. Figure 5 illustrates the variation in velocity resulting from changes in the number of blades.

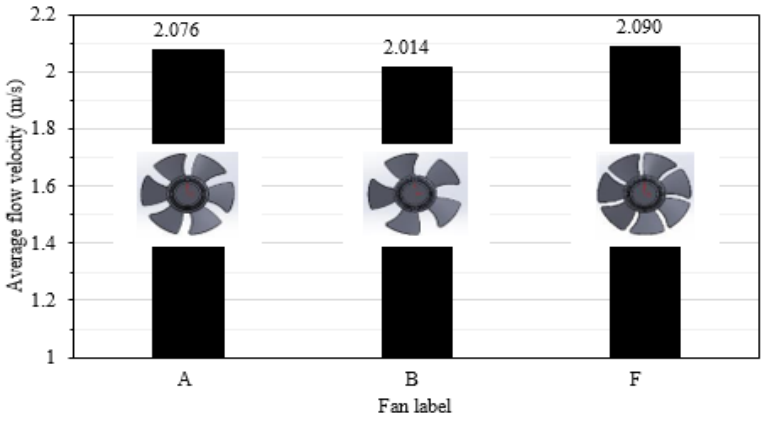

Figure 5. Average flow velocity for fans with different blade numbers

Development Shape of Blade

The effect of blade shape on fan performance was evaluated by applying eight distinct geometric modifications to the basic fan model (F). Model F was adopted based on the number of blades. The blade shape was changed while the fan diameter (hup, tip) was fixed. The resulting fan designs are classified from Fb1 to Fw,t2, as shown in Table 4. The geometric modifications applied to fan F included blade cuts on both sides in model Fb1 and arc-shaped cuts in model Fb2, while model Fw included the addition of a wing to the blade, increasing the air intake velocity. Therefore, the wing was fixed and subsequent modifications were made. With the wing fixed, the arc-shaped blade cut was applied to model Fw,b to achieve superior aerodynamic performance. Model Fw,s1 featured a single internal slit on the blade, while Fw,s2 featured a double internal slit, and Fw,t1 featured a single external projection on the blade surface. This was replicated on model Fw,t2 with a double external projection. Most of these modifications were made based on what was proposed in previous studies.

Table 4. Blade shape developments

Case No	Name	Ave. velocity – inlet (m/s)	percentage of improvement %	Fan developments	blade shape
1	Fb1	1.886	0		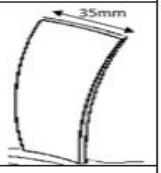
2	Fb2	2.089	1%	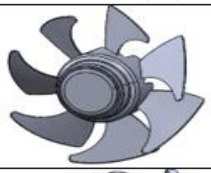	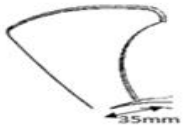
3	Fw	2.128	2.5%		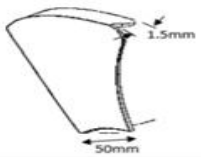
4	Fw,b	2.140	3.5%		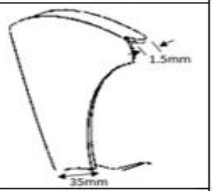
5	Fw,s1	2.106	1.5%	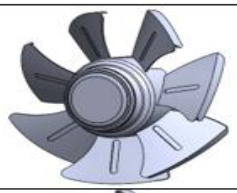	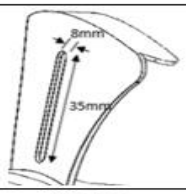
6	Fw,s2	2.099	1%	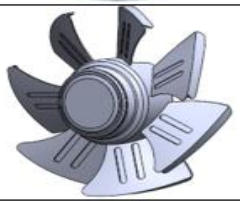	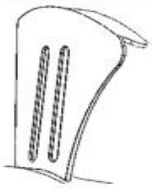
7	Fw,t1	2.025	0		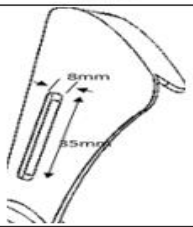
8	Fw,t2	2.088	0.9%		

Shroud Development

Blade tip clearance and shroud exit angles play a vital role in fan performance. A well-designed shroud reduces tip leakage by ensuring tight clearances, and exit angles reduce pressure loss, improving efficiency and enhancing flow velocity. Figure shows the dimensions and angles at which the shroud was developed. In this section, nine shroud configurations, labeled S1 to S9 (as given in Table), It was developed in conjunction with the fan configuration Fw, b to determine the optimal flap design and maximize aerodynamic performance. For clarity, the resulting configurations, S1 + Fw, b to S9 + Fw, b, are called configurations C1 to C9, respectively.

Table 5. Develop the shroud using tip clearance and shroud exit angle

Fan and shroud label	configu ration	Tip clearance (cm) (TC)	Exit angles for the shroud(α)	Average inlet velocity (m/s)	shroud shape
Fw,b + S2	C2	0.5	0	2.047	
Fw,b + S3	C3	0.3	0	2.016	
Fw,b + S4	C4	1	0	2.119	
Fw,b + S5	C5	1	14	2.277	
Fw,b + S6	C6	1	26.5	2.176	
Fw,b + S7	C7	1.3	19.5	2.322	
Fw,b + S8	C8	1.3	26.5	2.260	
Fw,b + S9	C9	1.5	14	2.113	

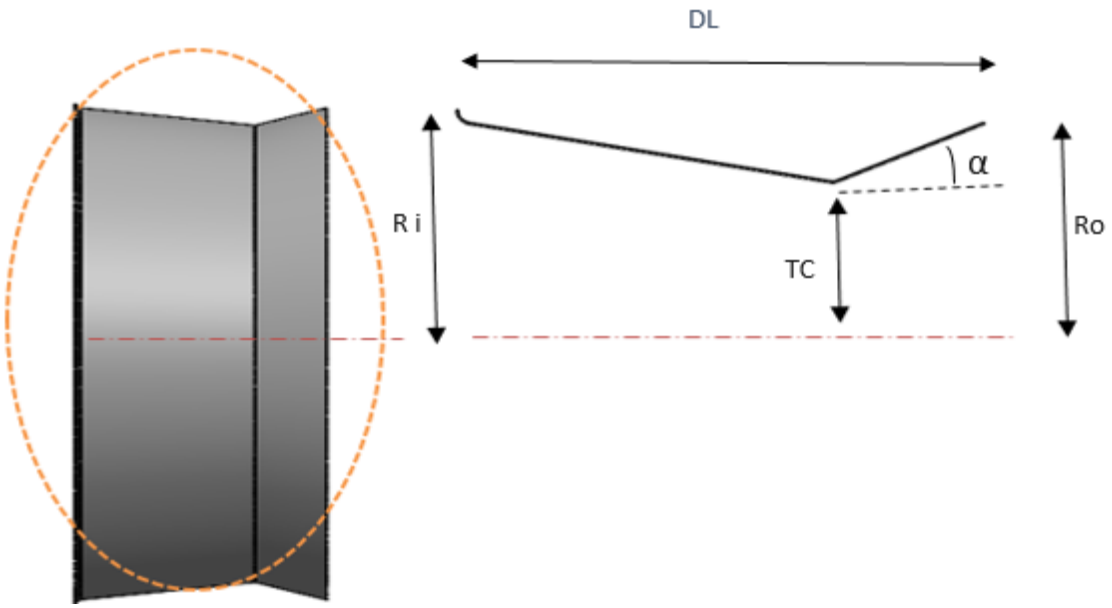

Figure 7. The dimensions and angles through which the shroud was developed, Ri, Ro are the air inlet and outlet diameter of shroud, respectively, TC is the tip clearance, and α is the angle

Results and Discussion

The following sections discuss opportunities to increase fan performance, specifically airflow velocity, by optimizing important design parameters, including the number and geometry of blades and the shroud configuration. The fan described in Table 1 is considered as the baseline model. Geometry modifications are done in two stages: first, adjusting the number of blades to identify the configuration that yields optimal flow development; second, assessing different blade shapes based on the optimized blade count.

Model Validation

The simulation outcomes generally align well with experimental data for the flow velocity of the baseline fan, as illustrated in Figure presents data obtained at the 17 points. Minor discrepancies are observed between the simulation and experimental results at certain locations, with the simulations slightly underestimating the flow rate. These marginal differences are likely due to the limitations of the state solver, which may not effectively capture the unsteady flow characteristics.

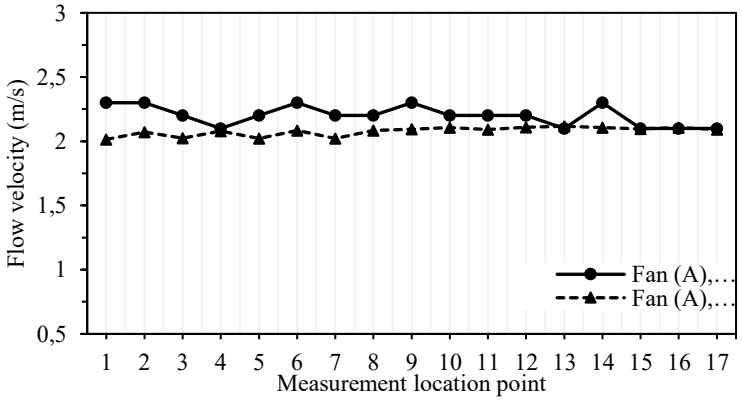

Figure 8. Experimental and numerical airflow velocity measurements taken at 17 different locations at the duct inlet.

Blade Shaps Assessment

Table shows the performance data for fan models Fb1 to F w, t2 at a fixed tip clearance of 0.7 cm, including average flow velocity and flow rate. As shown in Figure , the F w, b configuration achieved the highest performance among all eight blade designs studied, while the Fb1 configuration recorded the lowest performance

Table 6. Average flow velocity and flow rate for various fan configurations at a fixed tip clearance of 0.7 cm

Fan label	No. blades	Tip clearance (cm)	Average inlet velocity (m/s)	Flow rate (m^3/s)
Fb1	7	0.7	1.886	0.203
Fb2	7	0.7	2.089	0.225
F w	7	0.7	2.128	0.229
F w, b	7	0.7	2.140	0.230
Fw,s1	7	0.7	2.106	0.227
Fw,s2	7	0.7	2.099	0.226
Fw,t1	7	0.7	2.025	0.218
Fw,t2	7	0.7	2.088	0.225

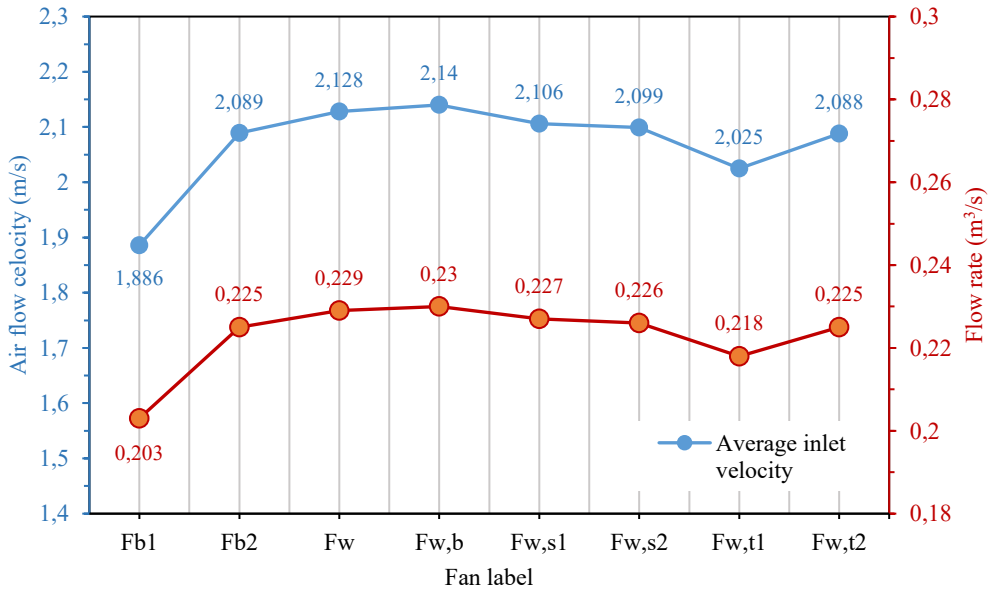

Figure 9. Average flow velocity and flowrate for the all-fan designs at a constant tip clearance of 0.7 cm

Figure shows the flow velocity and pressure curves for the basic fan (A) and the optimized configuration (Fw, b), both coupled with the standard shroud (S1). The results show a significant improvement in flow velocity consistency of approximately 3.5% across the inlet section when using Fw, b. This increase is observed in Figure (b) compared to Figure a and is primarily attributed to the improved fan configuration. As a result of this improvement, the Fw,b fan was chosen to further improve performance through optimized shroud configurations.

Shroud Assessment

Figure 6 shows the results of the analysis of the average flow velocity and flow rate for the various fan-combinations studied, Table details the combinations considered. The results indicate that the C7 combination achieved the highest performance, while the C3 recorded the lowest performance among all the combinations tested. This highlights that the S7 shroud achieves the most efficient coupling with the Fw,b fan, while the S3 shroud achieved the lowest performance. The average flow velocities achieved in the C7 and C3 configurations were 2.322 m/s and 2.016 m/s, respectively, indicating that improving the shroud design from S1 to S7 increases airflow by more than 11%.

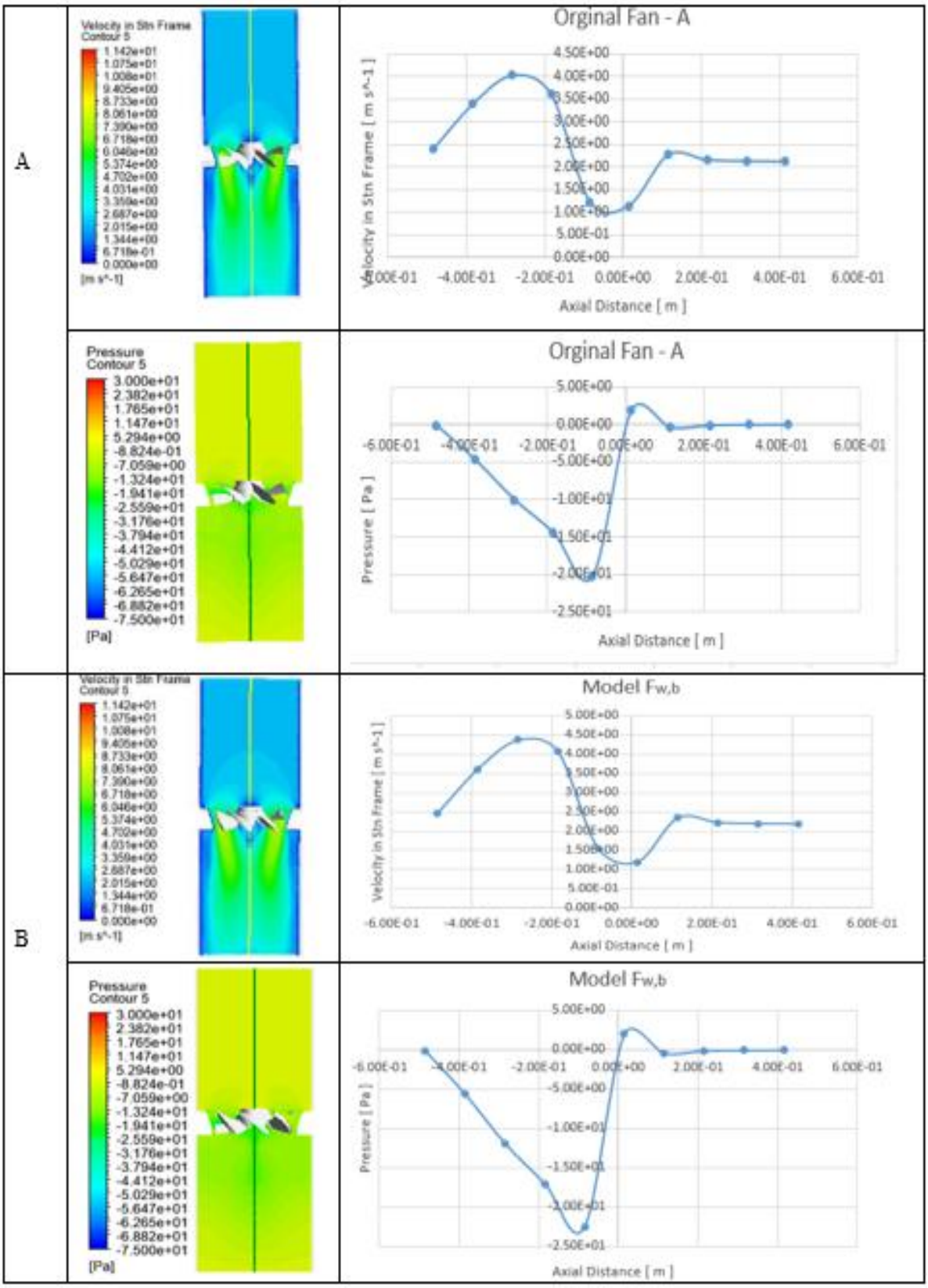

Figure 10. Velocity and pressure contours distribution, (a) Base line fan (A) + standard shroud (S1), (b) Model (F w, b) + standard shroud (S1)

Table 7. shows the performance data for fan shroud configurations S1 through S9 at different tip clearance dimensions and shroud exit angles.

Fan and shroud label	No. blades	Tip clearance (cm)	Exit angles for the shroud	Average inlet velocity (m/s)	Flow rate (m^3/s)
C1	7	0.7	0	2.140	0.230
C2	7	0.5	0	2.047	0.220
C3	7	0.3	0	2.016	0.217
C4	7	1	0	2.119	0.228
C5	7	1	14	2.277	0.245
C6	7	1	26.5	2.176	0.234
C7	7	1.3	19.5	2.322	0.250
C8	7	1.3	26.5	2.260	0.244
C9	7	1.5	14	2.113	0.228

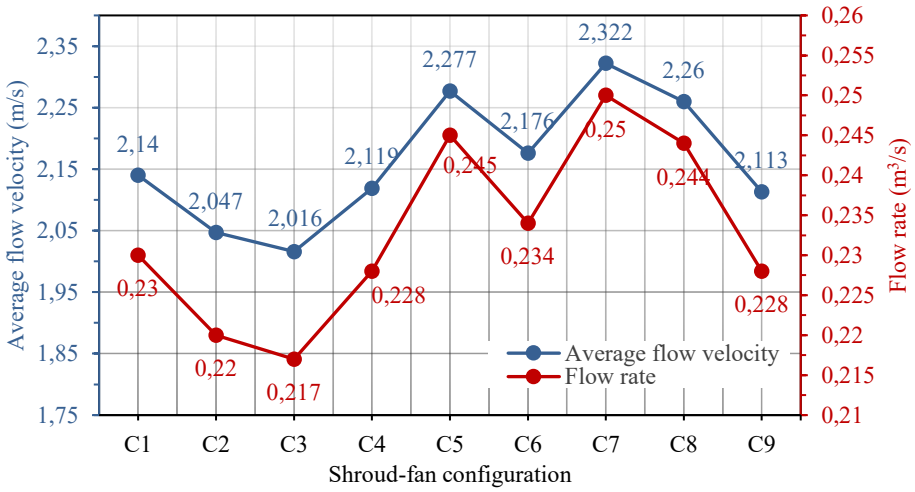

Figure 6. The analysis of the average flow velocity and flow rate

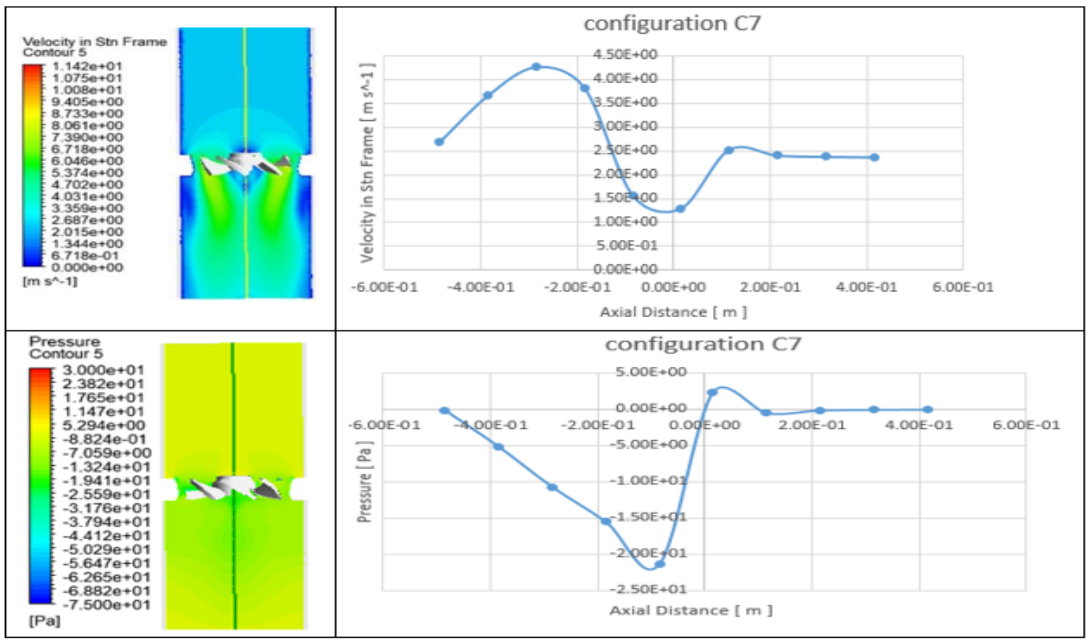

Figure 12. Velocity and pressure contours distribution, configuration C7

Figure shows the flow velocity and pressure curves for the improved fan (F w, b) coupled with the standard shroud (S1) and the improved shroud (S7), the data confirms a significant increase in flow velocity. This increase is mainly attributed to the improved shroud design.

Conclusions

This study provided a comprehensive analysis of fundamental geometric parameters influencing the performance of a small-scale axial flow fan, using both experimental measurements and validated CFD simulations. The experimental setup involved an open duct with a centrally placed axial fan, where flow measurements were taken at 17 inlet points. Developed numerical model based on the RANS equations with the SST k–ω turbulence model showed excellent agreement with experimental data, confirming its suitability for fan design optimization. The integration of numerical and experimental approaches enabled precise assessment and optimization of blade and shroud configurations. The following key findings were obtained:

- The 7-blade fan configuration demonstrated greater aerodynamic performance compared to the baseline 6-blade and proposed 5-blade designs.
- Improving the seven-blade fan with eight distinct blade geometries increased performance by 3.5%.
- Combining the optimal 7-blade fan with various shroud configurations identified the most effective shroud configuration which produced up to a 11% increase in flow velocity.

These findings contribute to the development of axial fan design by offering a validated methodology for enhancing performance.

Recommendations

To further enhance the performance of axial flow fans, it is recommended to focus more on reducing aerodynamic losses. Design optimization should consider additional parameters such as Changing the diameter of the hub relative to the tip diameter of the axial fan and changing the air entry angle of the fan shroud to improve flow uniformity and efficiency. Future studies should link experimental measurements with advanced CFD analysis to better comprehend the complex behavior and guide the development of high-efficiency designs. Furthermore, integrating modern design tools with manufacturing technologies can support the implementation of more effective aerodynamic improvements.

Scientific Ethics Declaration

* The authors declare that the scientific ethical and legal responsibility of this article published in EPSTEM Journal belongs to the authors.

Conflict of Interest

* The authors declare that they have no conflicts of interest

Funding

* This research received no external funding.

Acknowledgements or Notes

* This article was presented as View online at the International Conference on Engineering and Advanced Technology (ICEAT) held in Selangor, Malaysia on July 23-24, 2025.

* The authors would like to thank the conference organizers

* The authors thank the reviewers for their valuable feedback

References

Akwa, J. V., da Silva Júnior, G. A., & Petry, A. P. (2012). Discussion on the verification of the overlap ratio influence on performance coefficients of a Savonius wind rotor using computational fluid dynamics. *Renewable Energy*, *38*(1), 141–149.

Amin, G., Salunkhe, P., & Kini, C. (2024). Numerical analysis of a novel casing treatment in an axial flow fan. *Journal of Propulsion and Power*, *40*(6), 818–832.

Chen, Y., Liu, R., Peng, W., & Chen, S. (2025). Flow characteristics and loss mechanism of tip leakage flow in mining contra-rotating axial flow fan. *Applied Sciences*, *15*(4), 2232.

Corsini, A., Delibra, G., Rispoli, F., & Sheard, A. G. (2015). Aeroacoustic assessment of leading edge bumps in industrial fans. *FAN 2015-International Conference on Fan Noise, Technology and Numerical Methods*. Chromeextension://efaidnbmnnnibpcajpcglclefindmkaj/https://www.fan2025.org/archives/fan2015/papers/fp-pdf-86-CORSINI.pdf

Dragomirescu, A. (2011). Performance assessment of a small wind turbine with crossflow runner by numerical simulations. *Renewable Energy*, *36*(3), 957–965.

Kong, C., Wang, M., Jin, T., & Liu, S. (2023). The blade shape optimization of a low-pressure axial fan using the surrogate-based multi-objective optimization method. *Journal of Mechanical Science and Technology*, *37*(1), 179–189.

Liu, S., Guo, Y., Zhang, Y., Gu, C., & Yang, L. (2023). Effects of tip clearance and impeller eccentricity on the aerodynamic performance of mixed flow fan. *Symmetry*, *15*(1), 201.

Meyer, T. O., van der Spuy, S. J., Meyer, C. J., & Corsini, A. (2022). Optimization of a tip appendage for the control of tip leakage vortices in axial flow fans. *Journal of Turbomachinery*, *144*(10), 101006.

Moghadam, S. M. A., Meinke, M., & Schröder, W. (2019). Analysis of tip-leakage flow in an axial fan at varying tip-gap sizes and operating conditions. *Computers & Fluids*, *183*, 107–129.

Neshat, M. A. (2024). *CFD study of the leakage flow in low-speed axial-fans with rotating shroud* (Doctoral dissertation). Genova, Italy. https://tesidottorato.depositolegale.it/handle/20.500.14242/122005

Ostos, I., Ruiz, I., Gajic, M., Gómez, W., Bonilla, A., & Collazos, C. (2019). A modified novel blade configuration proposal for a more efficient VAWT using CFD tools. *Energy Conversion and Management*, *180*, 733–746.

Park, K., Choi, H., Choi, S., & Sa, Y. (2019). Effect of a casing fence on the tip-leakage flow of an axial flow fan. *International Journal of Heat and Fluid Flow*, *77*, 157–170.

Qiao, C., Ye, X., Wu, Y., & Li, C. (2025). Insight into the impact of blade perforation on the aerodynamics and acoustics of a two-stage variable-pitch axial fan. *Energies*, *18*(8), 1966.

Roy, S., & Saha, U. K. (2013). Review on the numerical investigations into the design and development of Savonius wind rotors. *Renewable and Sustainable Energy Reviews*, *24*, 73–83.

Ryu, S.-Y., Cheong, C., Kim, J. W., & Park, B. I. (2024). Analysis of aerodynamic and aeroacoustic performances of axial flow fans with variable winglet curvature in chordwise direction. *Results in Engineering*, *21*, 101857.

Sharma, S., & Sharma, R. K. (2016). Performance improvement of Savonius rotor using multiple quarter blades–A CFD investigation. *Energy Conversion and Management*, *127*, 43–54.

Sun, T., Wu, X., Mao, K., Wang, Z., Yang, H., & Wei, Y. (2024). Aerodynamic performance and flow optimization of axial fan based on the neural network and genetic algorithm. *Proceedings of the Institution of Mechanical Engineers, Part A: Journal of Power and Energy*, *238*(7), 1129–1147.

Tutar, M., & Cam, J. B. (2025). Computational design of an energy-efficient small axial-flow fan using staggered blades with winglets. *International Journal of Turbomachinery, Propulsion and Power*, *10*(1), 1.

Vala, J. R., Patel, D., Darji, A. P., & Balaji, K. (2024). *Numerical and experimental analysis of tip clearance effect of low-speed axial flow fan*. SAE Technical Paper.

Yadegari, M., Ommi, F., Aliabadi, S. K., & Saboohi, Z. (2024). Reducing the aerodynamic noise of the axial flow fan with perforated surface. *Applied Acoustics*, *215*, 109720.

Author(s) Information

Saddam Mansi
Al-Furat Al-Awsat Technical University, Technical College, Dept. of Power Mechanical Engineering Technology, Al-Musayab, Musayab, Iraq
Contact e-mail: *saddam.abdhussein.tcm86@student.atu.edu.iq*

Balasem Abdulameer Jabbar
Al- Furat Al-Awsat Technical University, Dept. of Mechanical Engineering Techniques of Power, Engineering Technical College of Najaf, Najaf 31001, Iraq.

To cite this article:

Mansi, S., & Jabber, B. A. (2025). Effect of blades shape and duct geometrical parameters on Aerodynamic performance of a small-sized axial fan. *The Eurasia Proceedings of Science, Technology, Engineering and Mathematics (EPSTEM), 37,* 614-628.